OFFICE OF SCIENTIFIC RESEARCH & DEVELOPMENT
NATIONAL DEFENSE RESEARCH COMMITTEE.
DIVISION SIX-SECTION 6.1

WATER TUNNEL TESTS
OF THE

7.2 CHEMICAL ROCKET.

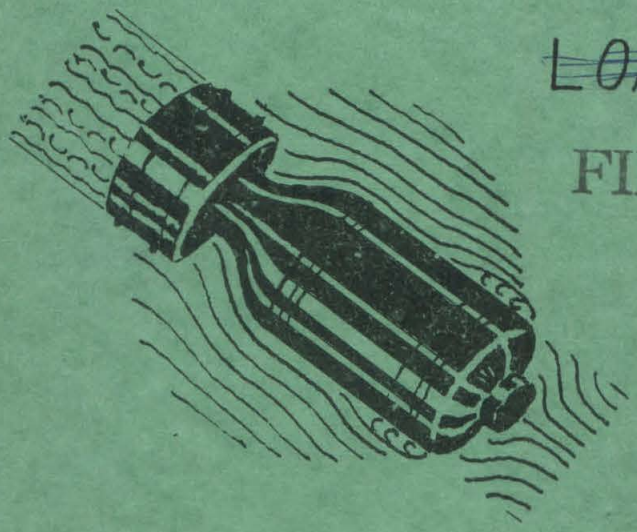

THE HIGH SPEED WATER TUNNEL
CALIFORNIA INSTITUTE OF TECHNOLOGY
PASADENA, CALIFORNIA.

SECTION Nº 6.1 - Sr-207-1261
HML REP. Nº ND-22.

COPY Nº 106

OFFICE OF SCIENTIFIC RESEARCH AND DEVELOPMENT
NATIONAL DEFENSE RESEARCH COMMITTEE
DIVISION SIX – SECTION 6.1

WATER TUNNEL TESTS OF THE 7.2" CHEMICAL ROCKET

BY

ROBERT T. KNAPP
OFFICIAL INVESTIGATOR

THE HIGH SPEED WATER TUNNEL
AT THE
CALIFORNIA INSTITUTE OF TECHNOLOGY
HYDRAULIC MACHINERY LABORATORY
PASADENA, CALIFORNIA

Section No. 6.1-sr-207-1261

HML Rep. No. ND-22

Report Prepared By
H. L. Doolittle
Hydraulic Engineer

December 22, 1943

SUMMARY

This report covers tests of a 2" diameter model of the 7.2" Chemical Rocket to determine its performance and possible means of increasing stability and reducing dispersion.

The rocket was tested with the two original tails, the ring tail designated herein as No. 61 and the ring tail with extended fins designated No. 62. Three other tail designs were tested designated No. 63, No. 67, and No. 68. Of these, No. 67 was the only one that produced results superior to the No. 61 and No. 62 designs. This No. 67 Tail has extended fins similar to Tail No. 62 and projects beyond the nozzle about one diameter. Details of these tails are given in Figure 12.

Tail No. 62 gave a restoring moment 50% greater than Tail No. 61, and Tail No. 67 gave a restoring moment 45% greater than Tail No. 62, both values being for 5° yaw. It is believed that Tail No. 67 represents about the best that can be done in redesigning the tail, as it produced a fairly high moment, a very large center-of-pressure eccentricity, and only one of the five tails tested has a lower drag coefficient.

In this connection it should be noted that all the tails tested gave, without exception, adequate stability to the projectile to insure satisfactory flight after burning is completed. Therefore, the only benefit to be obtained from an increase in the stability above that produced by the original ring tail (No. 61) must come from whatever reduction it might effect in the dispersion occurring during the burning of the propellent.

Calculation of the period of oscillation of the projectile in flight, and the equivalent wave length, makes possible a comparison of projectile performance from the standpoint of dynamic stability. It can be shown that, for rockets with long burning times, the shorter the wave length for a given projectile, the less will be the dispersion. Using this measure of dispersion, Tail No. 67 would be expected to produce 15% less dispersion than Tail No. 62, and Tail No. 62, 18% less than Tail No. 61.

This investigation leads to the conclusion that the No. 61, No. 62, and No. 67 Tails will give a high degree of static stability and it is improbable that much more can be accomplished by a redesign of the tail. It is also a fact that the dynamic stability of the projectile cannot be materially improved if its present physical dimensions are to be retained. The conclusion must, therefore, be reached that the most effective means of lowering the dispersion of this rocket is by reducing the malalignment of the jet with the axis of the projectile and eliminating as far as possible asymmetry in the tail assembly.

WATER TUNNEL TESTS OF THE 7.2" CHEMICAL ROCKET

GENERAL

This report covers Water Tunnel tests of a 2" diameter model of the 7.2" Chemical Rocket, conducted at the Hydraulic Machinery Laboratory of the California Institute of Technology. This work was done at the request of the Chief of Ordnance under their existing NDRC Project at this laboratory. The purpose of the tests was to determine the performance of the rocket with different tail designs in order to find, if possible, the cause of the excessive lateral dispersion observed with this projectile. Complete tests were conducted on models with the two tail designs submitted and, also, on three additional designs embodying modifications that were thought to be advantageous.

The report includes curves showing performance characteristics and, also, flow drawings made in the Polarized Light Flume, all of which are discussed in detail. All drawings refer to the model of the prototype based on a scale ratio of 3.6.

Appendix "A" gives definitions of the terms used in this report as well as a brief discussion of the required conditions for stability in a projectile.

Appendix "B" gives a description of the Characteristic Chart which shows the relative performance of the projectile with each of the tails tested.

DESCRIPTION OF PROJECTILE

The photographs, Figures 1 to 4, show the models with the two original tail designs. Figures 5 to 10 show three other tail designs that were tested. Figure 11 is a detail drawing of the complete model and Figure 12 gives details of the five tail designs.

FIGURE 1 – MODEL WITH TAIL NO. 61

FIGURE 2
TAIL NO. 61

FIGURE 3 – MODEL WITH TAIL NO. 62

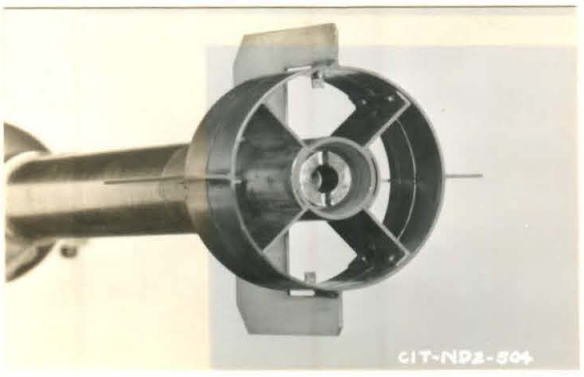

FIGURE 4
TAIL NO. 62

FIGURE 5

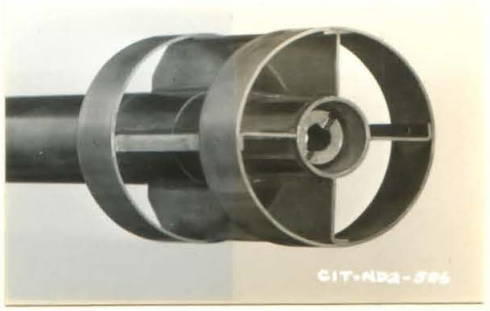

FIGURE 6

TAIL NO. 63

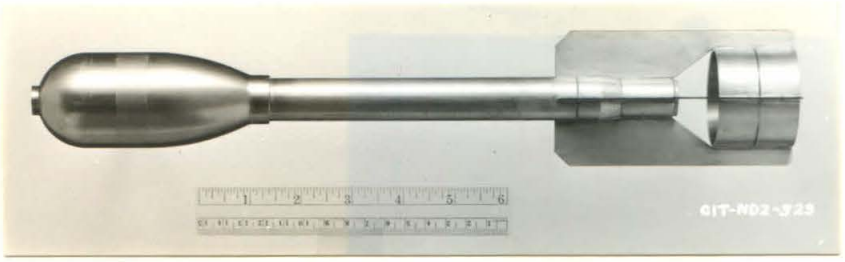

FIGURE 7

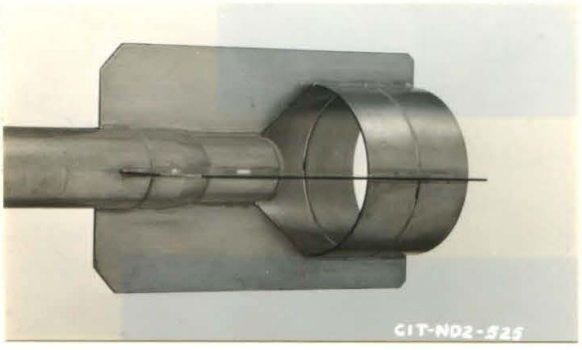

FIGURE 8

TAIL NO. 67

FIGURE 9

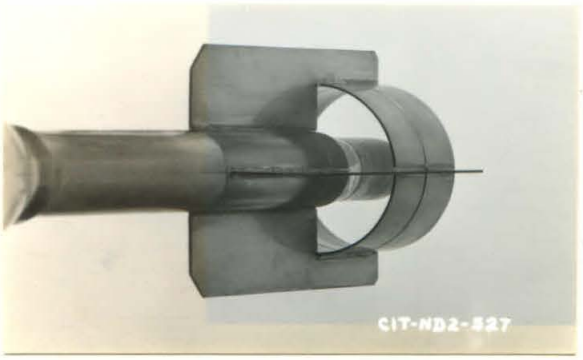

FIGURE 10

TAIL NO. 68

CONFIDENTIAL

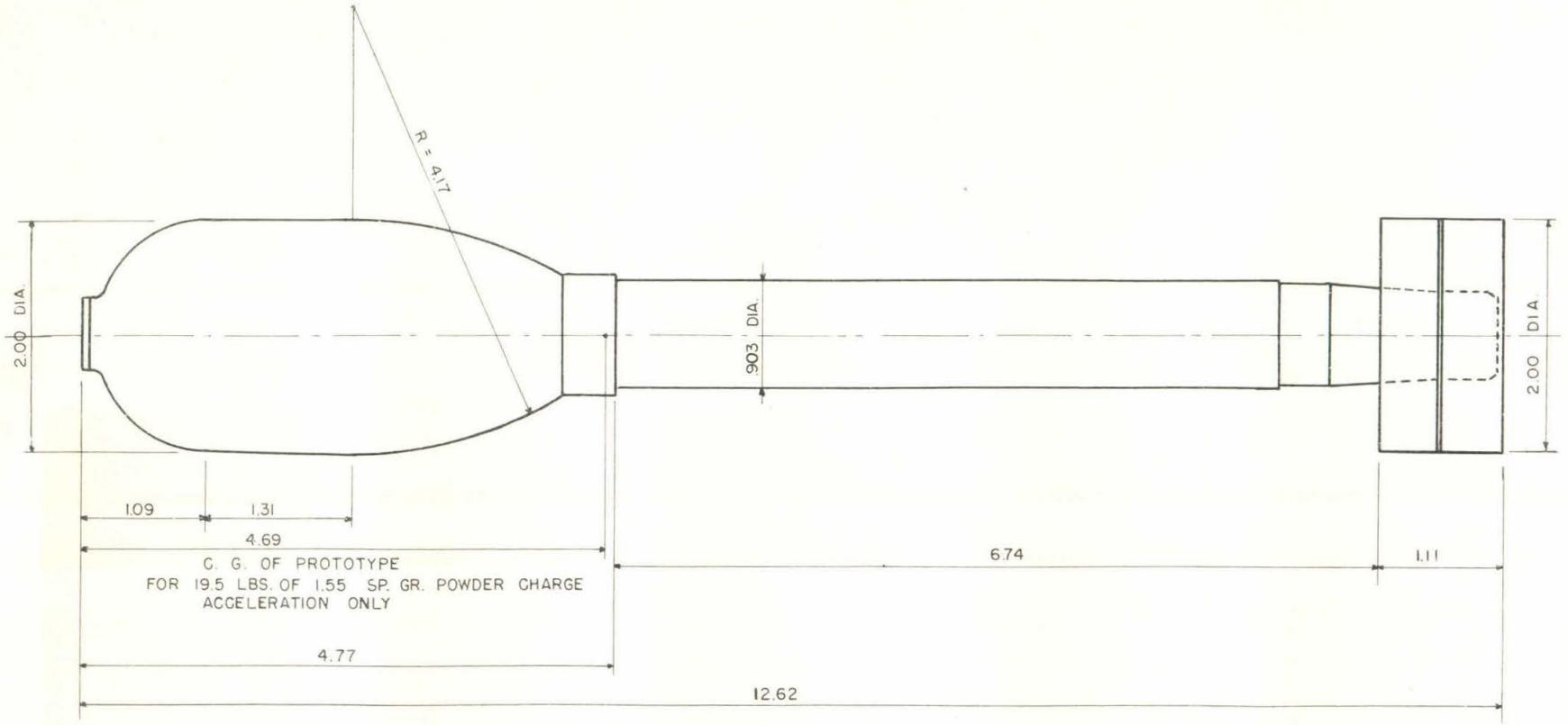

MODEL DETAIL
7.2" CHEMICAL ROCKET

MODEL SCALE 1: 3.6

CIT — HML
DRG. ND 22 - 2209M

FIGURE 11

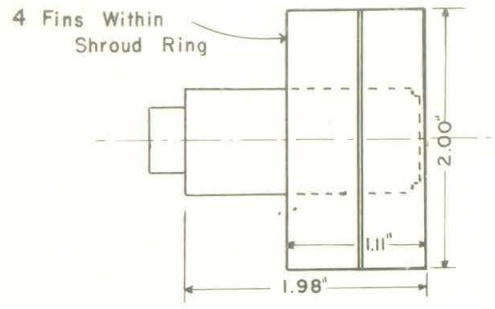

TAIL NO. 61

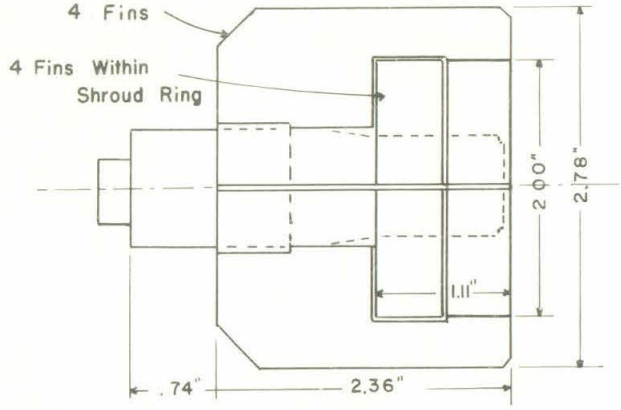

TAIL NO. 62

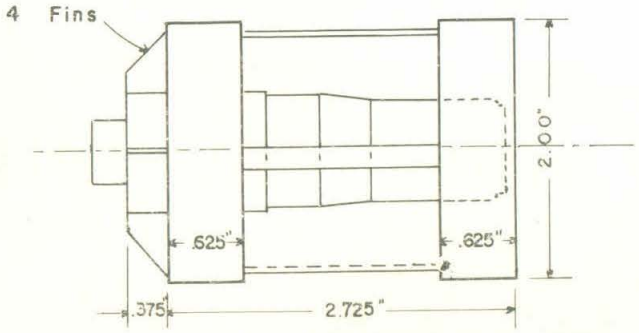

TAIL NO. 63

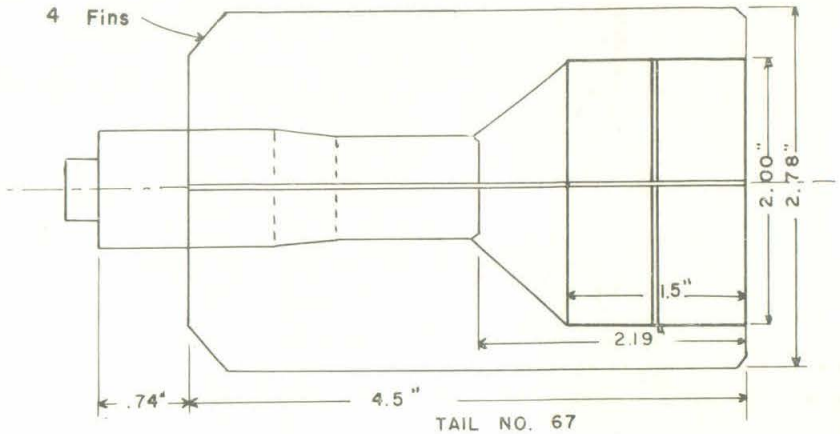

TAIL NO. 67

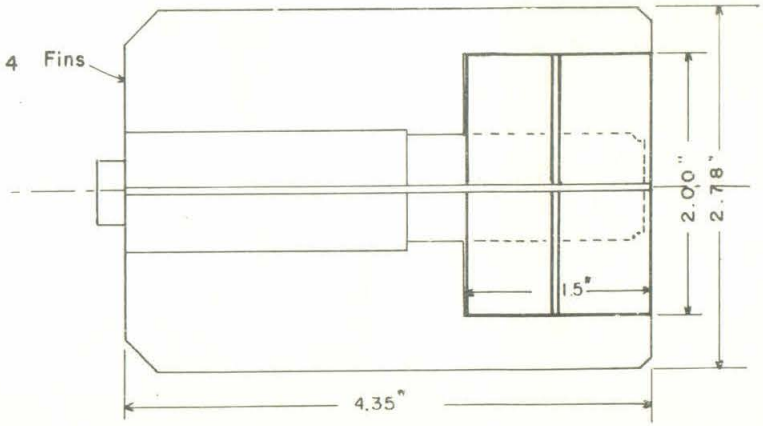

TAIL NO. 68

ALL DIMENSIONS REFER TO THE MODEL

MODEL SCALE 1:3.6

TAIL DETAILS

7.2" CHEMICAL ROCKET

CIT – HML
DRG. ND 22-2210M

FIGURE 12

CONFIDENTIAL

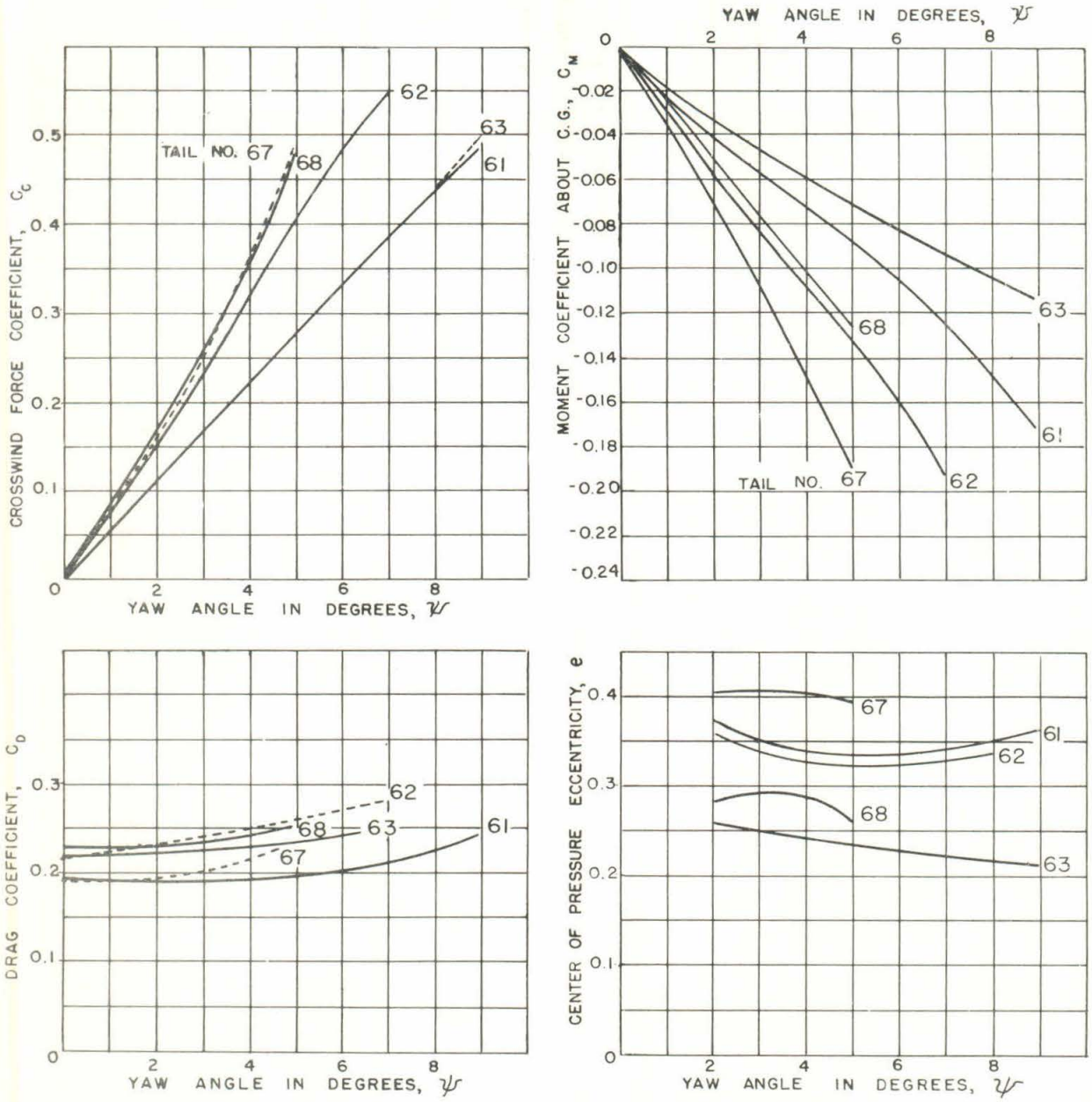

CURVES BASED ON POWDER DENSITY OF 1.55.
CURVES HAVE BEEN FAIRED AND CORRECTED FOR INTERFERENCE.

DRAG, CROSS FORCE AND MOMENT COEFFICIENTS

AND C.P. ECCENTRICITY

7.2" CHEMICAL ROCKET

CIT — HML
ND 22-1814M

FIGURE 13

PHYSICAL DATA FOR PROTOTYPE

Diameter	7.2"
Length from nose to end of nozzle	45.25"
Total weight excluding propellent and igniter	47.90 lbs
Explosive charge	19.5 lbs
Assumed specific gravity of explosive	1.55
C.G. distance from nose	17.70" or 0.391 L
Moment of inertia about C.G. calculated for above total weight	65.7 lb ft^2
Radius of gyration	14.0 inches

An effort was made to produce a satisfactory tail without the projecting fins, but, as the following discussion will show, this result was not attained. Tail No. 67 is quite similar to the original No. 62 Tail, with the exception of its location. As will be seen, this tail extends beyond the end of the nozzle a little more than one diameter. This overhang increases the stability materially and it is believed will result in no serious interference with the jet.

PERFORMANCE CHARACTERISTICS

In Figure 13 are shown performance curves for the rocket with five different tail assemblies. These curves give the variation of the drag, cross force, and moment coefficients, and, also, the center-of-pressure eccentricity with different yaw angles. It is seen that all of the models tested have a high degree of stability, as shown by the large values of the C.P. eccentricity and moment coefficient.

Of the two designs originally submitted, Tail No. 62 gives a much higher moment coefficient due to its greater outside diameter and the larger fin area, both of which, however, result in some increase in drag. Of the new tails tested, No. 67 is the one that produced the best results. At 5° yaw this tail gave a restoring moment about 45% greater than the No. 62 Tail and an increase of about 20% in the C.P. eccentricity. Tail No. 62, at 5° yaw, gave 50% greater restoring moment than Tail No. 61 and about the same C.P. eccentricity.

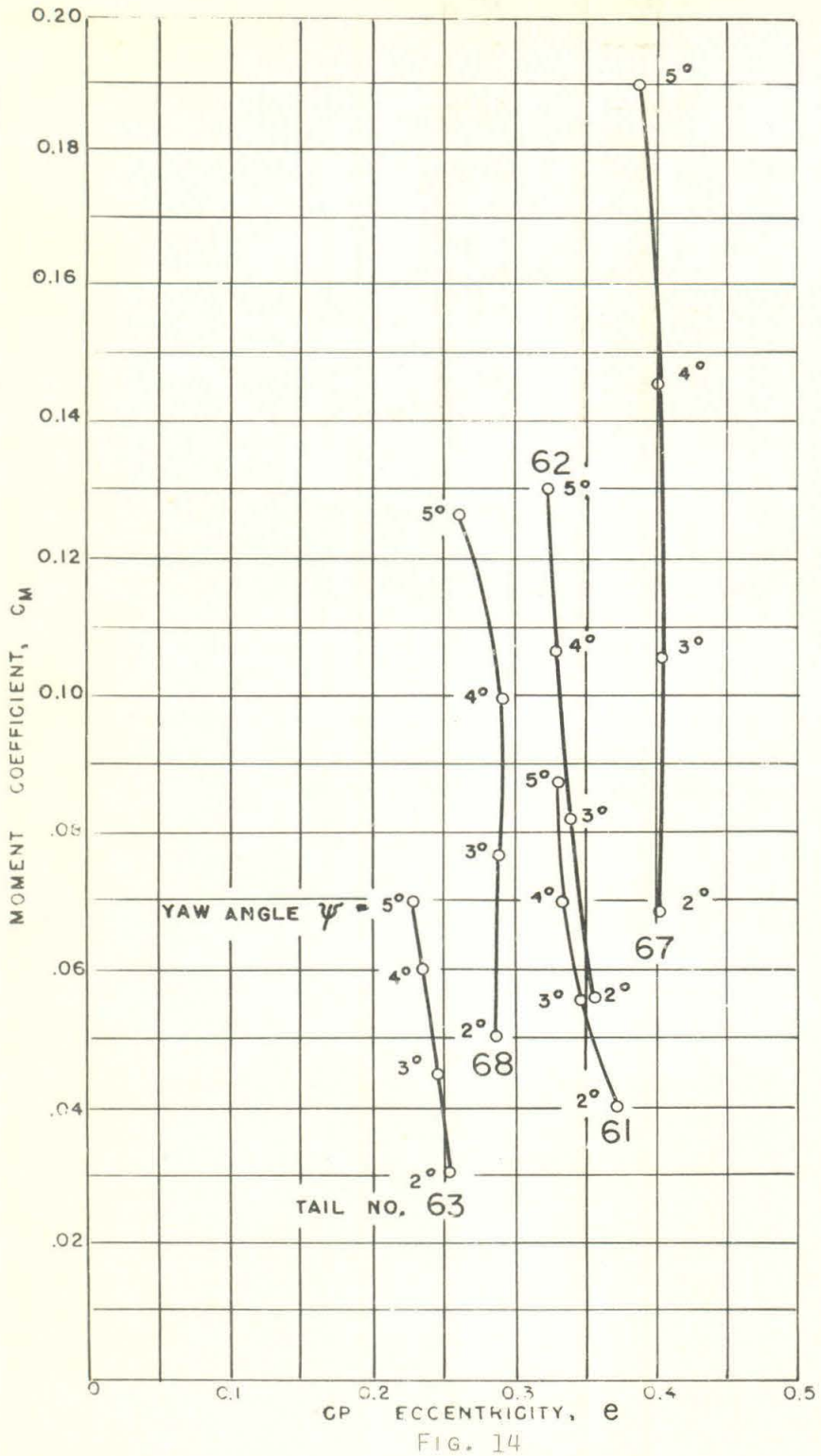

FIG. 14

Figure 14 shows the moment coefficient for the five tails plotted against the C.P. eccentricity. These curves indicate the relative merits of the various designs from the standpoint of static stability. On this basis, the projectile having the greatest restoring moment and the largest center-of-pressure eccentricity is the most stable.

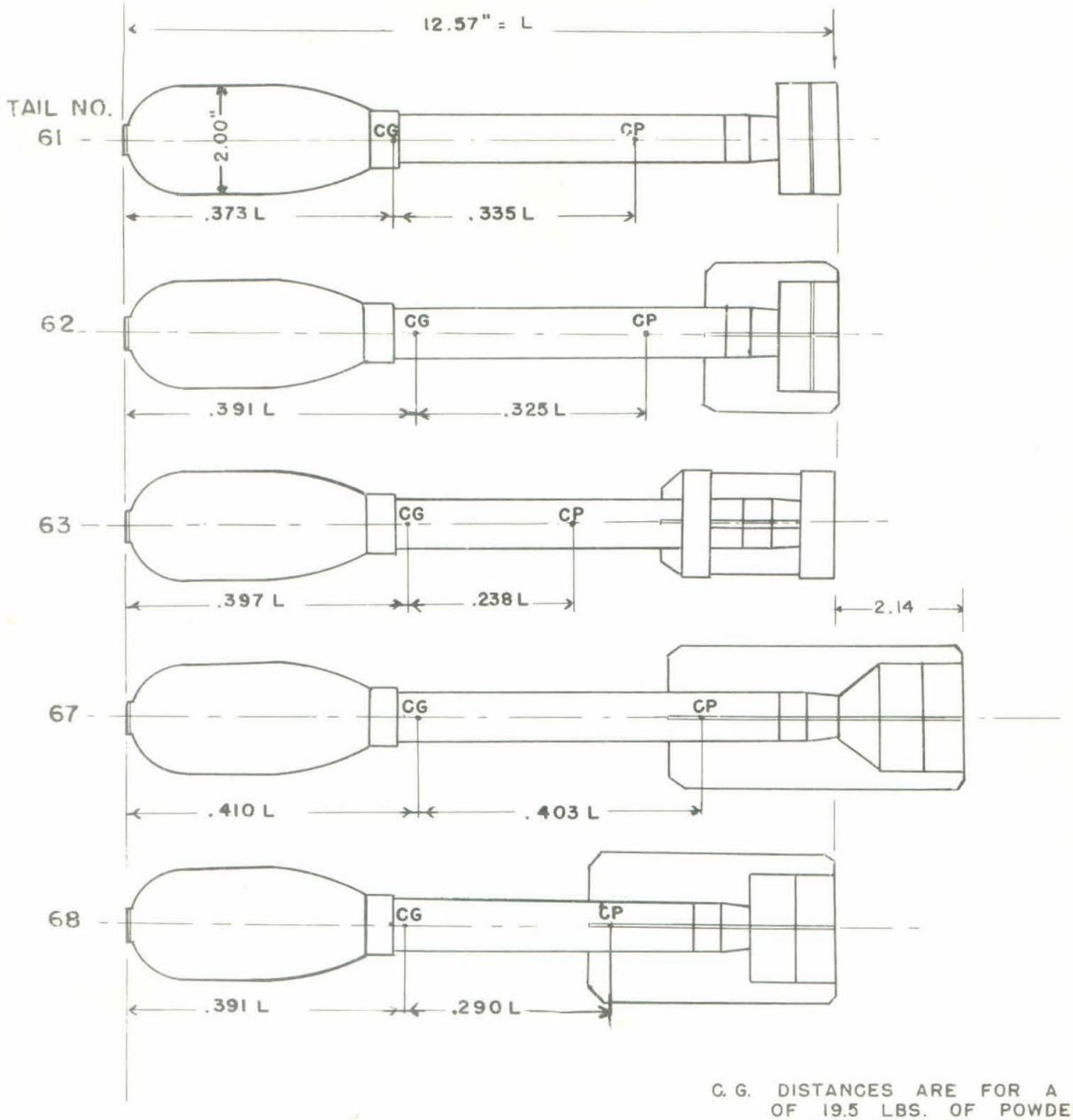

FIG. 15

C. G. DISTANCES ARE FOR A CHARGE OF 19.5 LBS. OF POWDER HAVING A SPECIFIC GRAVITY OF 1.55.

C. P. LOCATIONS ARE FOR 4° YAW ANGLE.

SEE FIG. 12 FOR TAIL DETAILS.

Figure 15 shows outlines of the projectile with the five tail designs. This gives the overall length, the center-of-gravity location, and the center-of-pressure location for a yaw of 4 degrees. The center of gravity has been calculated for a 19.5 lb. H. E. charge having a specific gravity of 1.55. The center-of-gravity location will, of course, change with the weight and specific gravity of the charge. An examination of Figure 14 shows that the center of pressure with Tail No. 67 remains practically in the same position as the yaw changes while with the other tails the C.P. shifts forward, reducing the C.P. eccentricity with increasing yaw.

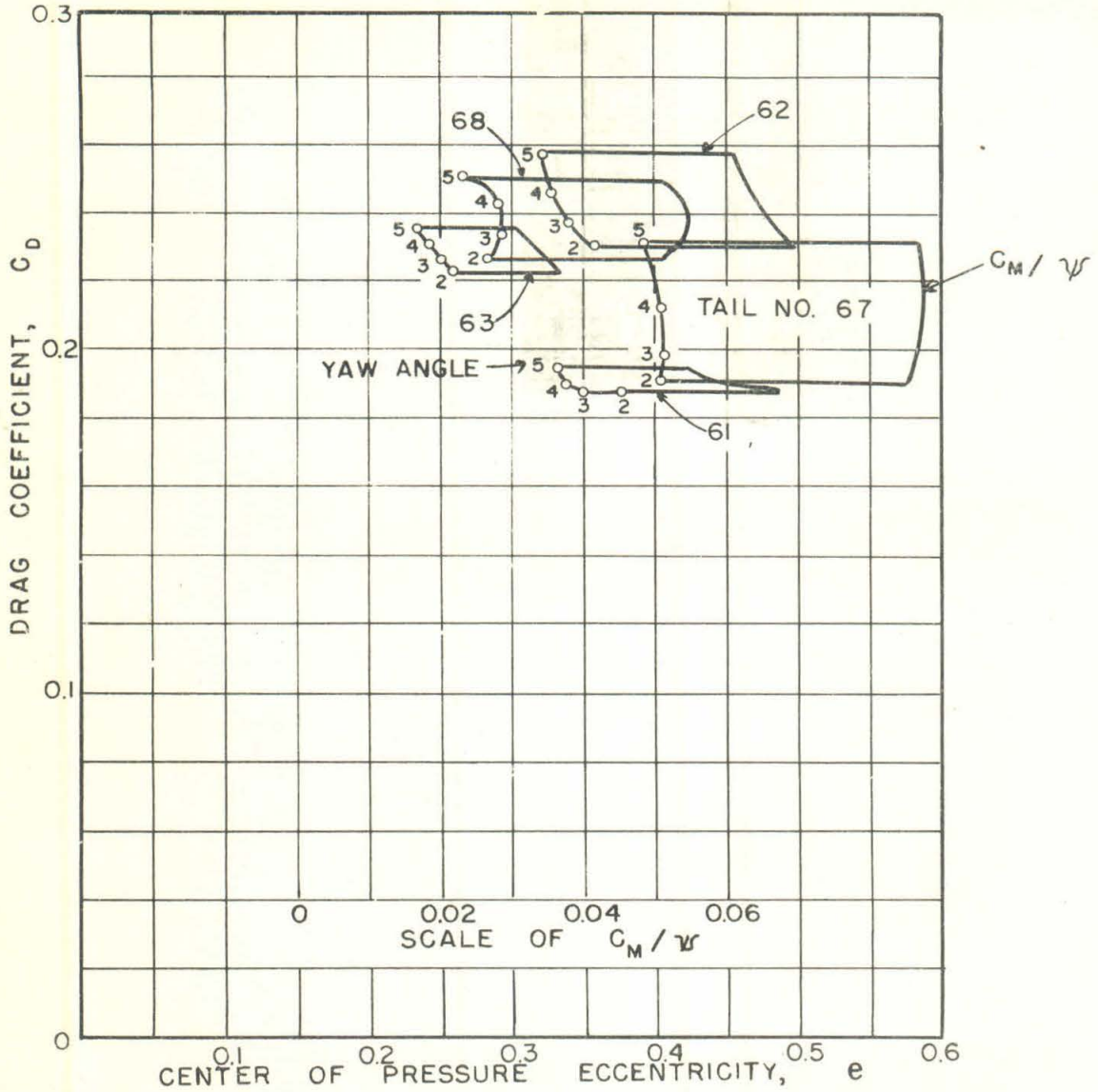

Fig. 16

CHARACTERISTIC CHART

The Characteristic Chart, Figure 16, provides another means of comparing the performance of the projectile with different tail designs. This chart shows the drag coefficient, the C.P. eccentricity, the rate of change of moment, and the yaw angle. Here, again, Tail No. 67 is shown to be superior to the other designs as it gives a low drag coefficient; the moment coefficient per degree of yaw remains practically constant and is greater than that with the other tails, also, it gives the greatest C.P. eccentricity.

Tail No. 67 has only four fins and no fins at all within the shroud ring, whereas Tail No. 62 has four fins outside of the shroud and four fins within the shroud. This difference in design no doubt accounts for most of the reduction in drag obtained with the No. 67 Tail.

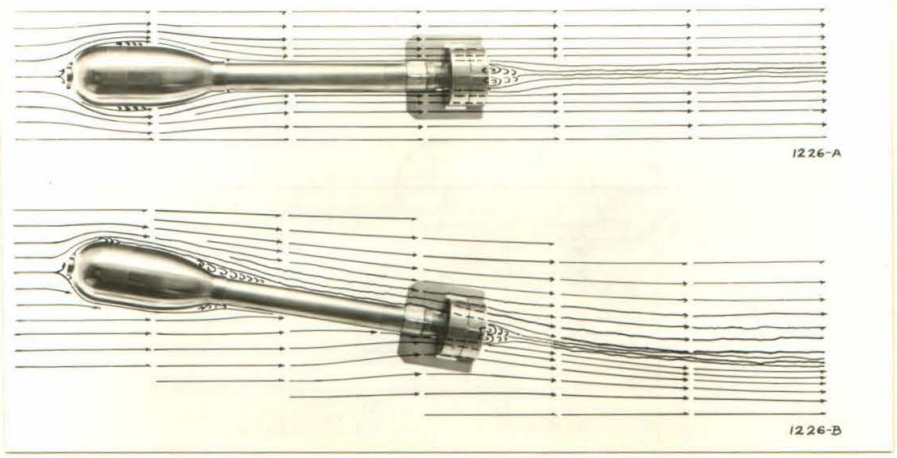

FIGURE 17
TAIL NO. 62

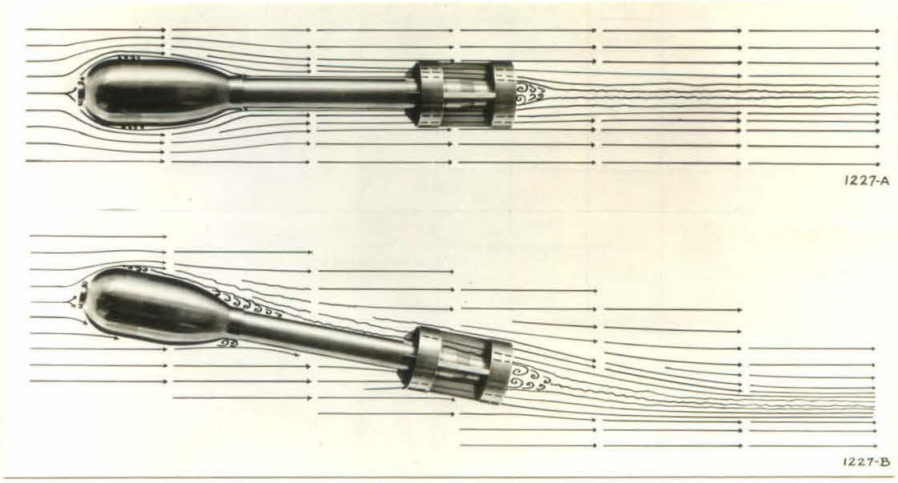

FIGURE 18
TAIL NO. 63

FLOW DRAWINGS

Figures 17 to 22 are drawings made from observations of the model in the Polarized Light Flume with the five tail designs. It is seen that the hemispherical nose causes only a slight disturbance of the flow. At the junction of the afterbody and the boom some disturbance is noticeable and this increases with the yaw angle.

The disturbance aft of the tail seems to be about the same for all tails and is probably due primarily to the square end of the nozzle. The most noticeable difference in flow for the five tail designs is in the amount of fluid deflected through the shroud ring. The greatest flow appears to be passing through the No. 67 Tail, probably due largely to the absence of fins and no blocking effect of the nozzle within the ring. This greater flow, no doubt, contributes much to the increase in moment produced by this tail, although the extra length of this design is also a factor in increasing the moment.

FLOW DRAWINGS

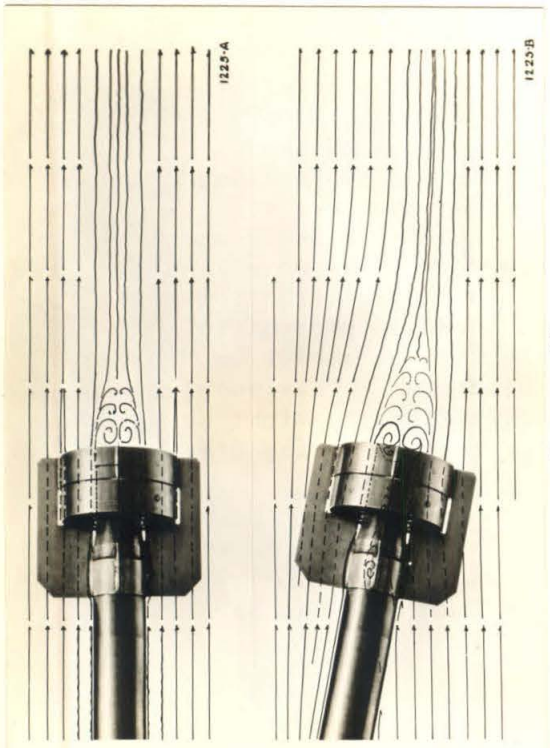

FIGURE 20
TAIL NO. 62

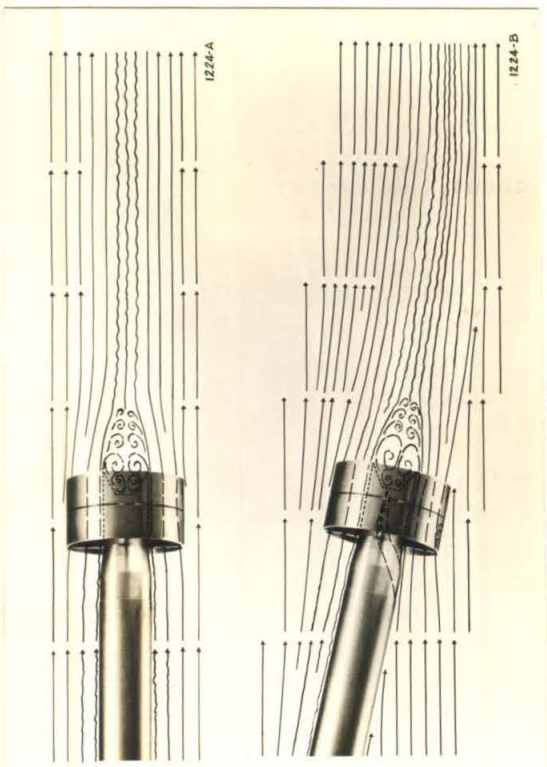

FIGURE 19
TAIL NO. 61

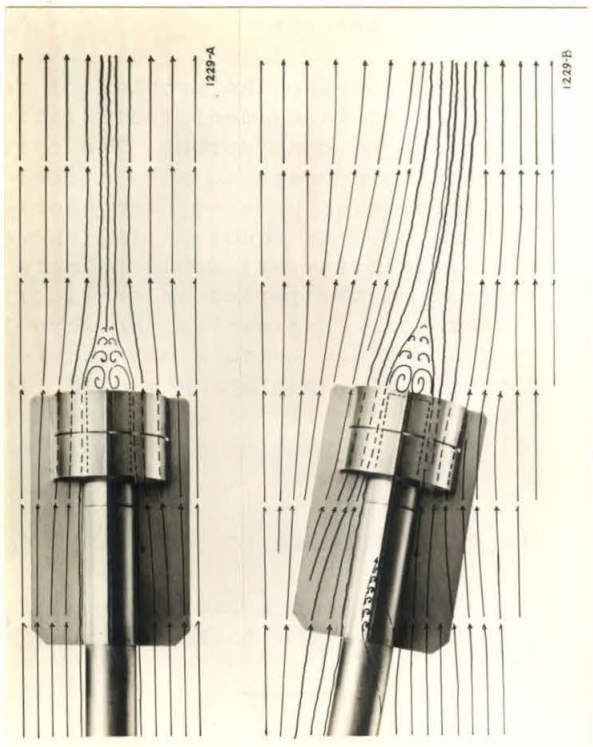

FIGURE 22
TAIL NO. 68

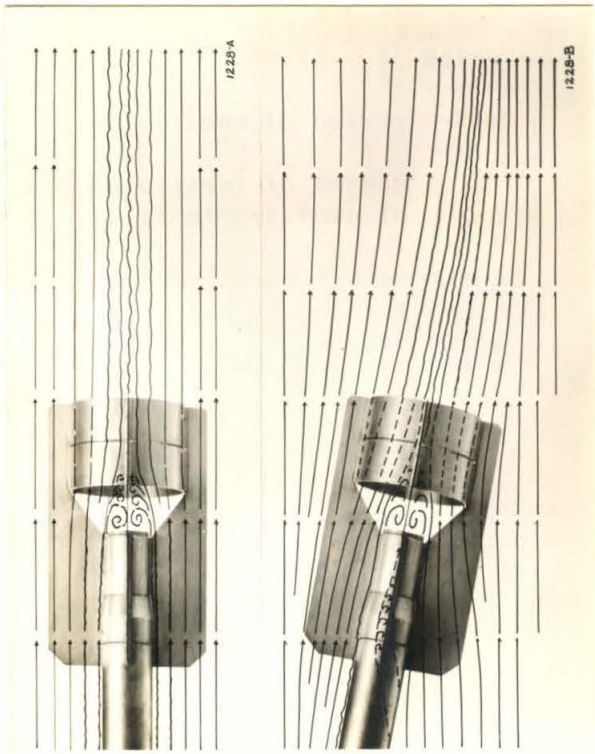

FIGURE 21
TAIL NO. 67

DYNAMIC STABILITY

In studying the problem of reducing the dispersion of projectiles it is evident that static stability is not the only factor to be considered. The period of oscillation of the projectile appears to have a decided effect on the dispersion, the relationship being, the shorter the period, the less the dispersion. As Equation (5) shows the wave length to be independent of the velocity, it would be more desirable to use the wave length instead of the period in considering the effect of oscillation on dispersion. Expressing the wave length in terms of projectile length gives a measure of dynamic stability that is useful in comparing the performance of different projectiles. This quantity, S/L, or the ratio of wave length to projectile length, might be called the parameter of dynamic stability, its value being given by Equation (6).

PERIOD OF OSCILLATION AND WAVE LENGTH

The period of oscillation of yaw, after burning, can be calculated by the following fundamental equation for harmonic motion:

$$T = 2\pi\sqrt{\frac{\frac{I}{g}}{-\frac{M}{\psi_o}}} \qquad (1)$$

in which

T = period of oscillation, seconds.

I = moment of inertia of projectile about the center of gravity, lb ft^2.

M = moment about the C.G., ft lbs.
(It is assumed that M varies directly with the angle of yaw)

ψ_o = angle of yaw, radians.

It should be borne in mind that the ratio, M/ψ_o, will be negative for a stable projectile because M and ψ_o must have opposite signs for stability. The expression under the radical will, therefore, be positive and T will have a real value. If the projectile is not stable, M/ψ_o will be positive, the expression under the radical will be negative, and T will be imaginary.

The value of the moment can be found from the equation for the moment coefficient as follows:

$$M = \frac{C_M \, A \, L \, W \, V^2}{2 \, g} \qquad (2)$$

where

C_M = moment coefficient obtained from tunnel tests.

A = area of cross section of projectile, sq ft.

L = length of projectile, ft.

W = specific weight of the fluid (air) in pounds per cu ft.

V = velocity of projectile, ft per sec.

g = acceleration of gravity.

Substituting this value of M in the equation for T and expressing the angle of yaw in *degrees* (ψ) instead of radians (ψ_o), we obtain

$$T = \frac{2\pi}{V}\sqrt{\frac{0.035 \, I}{-\frac{C_M}{\psi} \, A \, L \, W}} \qquad (3)$$

The wave length, S, is then found from the formula

$$S = V \, T \qquad (4)$$

or

$$S = 2\pi\sqrt{\frac{0.035 \, I}{-\frac{C_M}{\psi} \, A \, L \, W}} \qquad (5)$$

The wave length in terms of projectile length is, from Equation (5)

$$\frac{S}{L} = 2\pi\sqrt{\frac{0.035 \, I}{-\frac{C_M}{\psi} \, A \, L^3 W}} \qquad (6)$$

CALCULATION OF PERIOD AND WAVE LENGTH

By means of equations (3) and (4) the period for one complete oscillation and the corresponding wave length can be calculated,

using the following values for the properties of the projectiles:

I = 65.7 lb ft^2. This value for the moment of inertia was calculated for a charge of 19.5 lbs of explosive having a specific gravity of 1.55, the propellent and igniter not included.

V = 720 ft per sec. This is the velocity after burning taken from the NDRC report referred to above.

L = 3.77 ft.

A = 0.283 sq ft.

W = 0.075 lbs per cu ft for air.

The slopes of the moment coefficient curves are given by the following figures taken from the curves in Figure 13:

Tail No.	C_M	Yaw (ψ)	$C_{M/\psi}$
61	-0.16	8^o	-0.02
62	-0.18	6^o	-0.03
67	-0.22	5.4^o	-0.04

Substituting these values in the above equations the following values for period and wave length are obtained:

Tail No.	Period (T), Sec.	Wave Length, Ft.	Wave Length in Terms of Projectile Length
61	0.328	236	62.5 L
62	0.268	192	51.2 L
67	0.230	166	43.7 L

DISPERSION AND OSCILLATION

It is possible that the lateral displacement of the projectile due to oscillation might be one of the causes of dispersion. In order to arrive at the magnitude of this effect the maximum lateral displacement from the mean trajectory has been calculated for the oscillating projectile. This will be equivalent to the maximum dispersion due to this cause.

The maximum lateral displacement of an oscillating projectile from its mean trajectory is expressed by the following equation:

$$Y_{max} = \frac{C\ I\ \psi_o}{W_p\ M} \qquad (7)$$

Substituting in Equation (7) the values for the cross force and moment coefficients as given in Appendix A, we obtain:

$$Y_{max} = \frac{C_C\ I\ \psi_o}{W_p\ C_M\ L} \qquad (8)$$

in which

Y_{max} = maximum lateral displacement, feet.

C_C = cross force coefficient corresponding to ψ_o.

C_M = restoring moment coefficient corresponding to ψ_o.

W_p = weight of projectile, lbs.

ψ_o = maximum yaw angle, radians.

I = moment of inertia of the projectile about its C.G., lb ft^2.

L = length of projectile, ft.

Using the formula (8) and assuming the maximum yaw angle to be 5^o, the maximum displacement can be calculated for the projectile fitted with the five different tails. The values for the cross force and moment coefficients given below were taken from the performance curves in Figure 13.

Tail No.	Moment Coefficient C_M	Cross Force Coefficient C_C	Y_{max}, ft.
61	-0.088	0.28	0.10
62	-0.132	0.41	0.10
63	-0.072	0.28	0.12
67	-0.19	0.49	0.08
68	-0.126	0.48	0.12

It is believed these calculations give approximately correct values for the maximum displacement resulting from the oscillation of the projectile. From the above it is evident that dispersion

due to oscillation is negligible in this case and that the excessive dispersion noted with this projectile must be attributed to other causes.

DISPERSION AND BURNING TIME

An extensive investigation has been made of the various factors affecting the dispersion of rockets, the results of which are given in the NDRC Armor and Ordnance Report No. A-164, Division 3, entitled, "The Effects of Fin Size, Burning Time, and Projector Length on the Accuracy of Rockets." This report shows that, for rockets having malalignment of the jet, practically the entire effect on dispersion is produced within the time equal to the period of oscillation of the projectile and is roughly proportional to the burning time if this is less than the period. If the burning time exceeds the period, very little additional effect on the dispersion results during this additional time. In other words, it may be said that practically the entire effect on dispersion is produced in the distance equal to one-half wave length for one complete cycle of oscillation. If the burning distance is greater than this half wave length, very little *additional* effect on dispersion results.

The report just referred to gives the following data pertaining to this rocket:

Velocity after burning ceases = 720 ft per sec.

Time at which burning ceases = 0.47 sec.

$$\text{Burning distance} = \frac{720 \times 0.47}{2} = 169 \text{ ft.}$$

As noted previously in this report, the period of one oscillation of yaw, (T), and the corresponding half wave length, (S/2), for the projectile fitted with the No. 61, No. 62, and No. 67 Tails are as follows:

With Tail No. 61 T = 0.328 sec $\frac{S}{2}$ = 118 feet.

With Tail No. 62 T = 0.268 sec $\frac{S}{2}$ = 96 feet.

With Tail No. 67 T = 0.230 sec $\frac{S}{2}$ = 83 feet.

These figures show that the half wave length for the rocket fitted with the three tails noted varies from 50% to 70% of the burning distance. It is evident that this accounts, to some extent, for the better performance of the No. 62 Fin Tail and it is logical to expect that the No. 67 Tail would further decrease the dispersion.

It should not be forgotten that these statements rest on the assumption that the burning time and jet alignment remain unaffected by these changes. It naturally follows from this study that a decrease in the burning time, other factors remaining constant, will decrease the dispersion.

CONCLUSIONS

An analysis of the data herein leads to the conclusion that, from the standpoint of both static and dynamic stability, the No. 67 Tail design gives the best performance and that the No. 62 design is considerably better than the No. 61 design. Taking the wave length as the measure of dispersion, the No. 67 Tail would be expected to produce 15% less dispersion than the No. 62 Tail and the No. 62 Tail 18% less than the No. 61 Tail.

In considering the factors that affect dispersion the following statements appear to be justified when applied to rockets having no malalignment of the jet:

(a) The shorter the period of oscillation, the less the dispersion.

(b) The shorter the wave length for one complete oscillation, in terms of projectile length, the less the dispersion.

(c) The effect of the physical properties of the projectile on dispersion is disclosed by an examination of Equation (6). In order to reduce dispersion the value of S/L must be decreased. This can be done in the following ways:

(1) Reduce the moment of inertia

(2) Increase the moment coefficient

(3) Increase the diameter or length

Since the moment of inertia, diameter, and length are determined by the original design and are not subject to much variation, the only means left for bettering performance is increasing the moment coefficient by redesign of the tail.

In the NDRC Report No. A-164 above referred to, the following statement is made regarding tail design in its relation to dispersion:

"In cases in which - - - the projector length is less than one-fifth of the burning distance, the results (of the analysis) may be roughly summarized as follows: Fins of such size as to make the period of vibration equal to the burning time decrease the dispersion to about 70 percent of the dispersion with no fins,

or, more rigorously, with fins just large enough to give the rocket neutral stability. For fins of greater size the dispersion is roughly proportional to the period of oscillation in free flight produced by the fins."

The superior performance of the No. 67 Tail design with its large restoring moment illustrates what can be done by altering the tail to increase the moment coefficient and center-of-pressure eccentricity. As these two values are now quite high, it is believed little more can be done to better the performance by a change in the tail design.

For rockets having malalignment of the jet the dispersion will be affected by the amount of the malalignment and the burning time. It, therefore, appears that:

(d) The dispersion is directly proportional to the amount of malalignment of the jet.

(e) The dispersion is, roughly, directly proportional to the burning time within the interval equal to the period of oscillation. If the burning continues beyond this time little additional effect on the dispersion will result.

From paragraphs (d) and (e) it follows that the dispersion can be lowered by reducing the malalignment of the jet and by shortening the burning time. If it is not practicable to shorten the burning time an equivalent effect can be obtained by reducing the period of oscillation. However, shortening the period primarily for the purpose of reducing dispersion due to oscillation would not be justified as dispersion from this cause has been shown to be negligible in this case.

In summing up the results of this investigation it is seen that the restoring moment, the center-of-pressure eccentricity, the lateral displacement due to oscillation, and the burning time are all favorable to a low dispersion. It must, therefore, be concluded that any excessive dispersion is due to other causes, the most probable being malalignment of the jet or asymmetry of the tail. In connection with the former it is interesting to note the following statement taken from the NDRC No. A-164 Report:

"The inaccuracy of rockets arises primarily from the failure of the axis of the jet to pass through the center of mass of the projectile. This causes the rocket to rotate, during burning, about an axis through the center of mass perpendicular to the trajectory, with the result that the direction of thrust of the motor is changed from its initial direction as determined by the orientation of the rails."

Jet malalignment may be due not only to physical malalignment of the nozzle, but, also, to non-uniform velocity distribution

within the jet due to separation, shock waves, etc. within the throat and downstream section of the nozzle.

The importance of reducing, as far as possible, any asymmetry in the tail assembly cannot be over emphasized. This asymmetry produces a cross force which, with a non-rotating projectile, results in a drift in one direction only, thus increasing the dispersion.

THE HIGH SPEED WATER TUNNEL
AT THE
CALIFORNIA INSTITUTE OF TECHNOLOGY

APPENDIX A

DEFINITIONS

YAW ANGLE

The angle which the axis of the model makes with the direction of flow. Looking down on the model, yaw angles in a counter-clockwise direction are negative (-) and in a clockwise direction, positive (+).

MOMENTS

Moments tending to rotate the model in a counter-clockwise direction (when looking down on the model) are negative (-), and those causing clockwise rotation, positive (+).

In accordance with this sign convention a moment has a destabilizing effect when it has the same sign as the yaw angle.

In all model tests the moment is measured about the point of support.

Moments about the center of gravity have the symbol, M_{cg}.

DRAG

The force, in pounds, exerted on the model parallel with the direction of flow.

CROSS FORCE

The force, in pounds, exerted on the model normal to the direction of flow. A positive cross force is defined as one acting in the same direction as the displacement of the projectile nose for a positive yaw.

NORMAL COMPONENT

The sum of the components of the drag and cross force acting normal to the axis of the model. The value of the normal component is given by the following:

$$N = (D \sin \psi + C \cos \psi)$$

in which

N = Normal component in lbs

D = Drag in lbs

C = Cross force in lbs

ψ = Yaw angle in degrees

CENTER OF PRESSURE

The point in the axis of the model at which the resultant of all forces acting on the model is applied. This has the symbol (CP).

CENTER-OF-PRESSURE ECCENTRICITY

The distance between the center of pressure (CP) and the center of gravity (CG) expressed as a decimal fraction of the length (L) of the model. The center-of-pressure eccentricity (e) is derived as follows:

$$e = \frac{(L_{cp} - L_{cg})}{L} = \frac{1}{L} \quad \frac{M_{cg}}{N}$$

in which

e = Center-of-pressure eccentricity

L = Length of model in feet

L_{cg} = Distance from nose of projectile to CG in feet

L_{cp} = Distance from nose of projectile to CP in feet

COEFFICIENTS

The three force coefficients used are derived as follows:

Drag coefficient, $$C_D = \frac{D}{\rho \frac{V^2}{2} A_D}$$

Cross force coefficient, $$C_C = \frac{C}{\rho \frac{V^2}{2} A_D}$$

Moment Coefficient, $$C_M = \frac{M}{\rho \frac{V^2}{2} A_D L}$$

in which

D = Measured drag force in lbs

C = Measured cross force in lbs

ρ = Density of the fluid in slugs/cu ft

w = Specific weight of the fluid in lbs/cu ft

g = Acceleration of gravity in ft/sec^2

A_D = Area in sq ft of a cross section at the cylindrical portion of the projectile taken normal to the geometric axis of the projectile

V = Mean relative velocity between the water and the projectile in ft/sec

M = moment in foot-lbs measured about any particular point on the geometric axis of the projectile

L = overall length of the projectile in feet

GENERAL DISCUSSION

The curves of force and moment coefficients and of center-of-pressure distance plotted as functions of the yaw angle are useful for a discussion of the stability of projectiles. Since these tunnel tests are made under steady flow conditions, the results will only indicate the tendency of the projectile to return to or move away from the equilibrium position after a disturbance. Adopting aerodynamic usage, a projectile is said to be "statically" stable if it tends to return to equilibrium when disturbed. In the discussion of static stability the actual motion following the perturbation is not considered at all. In fact, a projectile may oscillate about the equilibrium position without ever remaining in it. In this case the projectile would be statically stable even though "dynamically" unstable. For a complete discussion of the mode of motion to be expected following a perturbation, the "dynamic" stability, additional information is necessary.

The condition for equilibrium is satisfied if C_M, calculated about the CG is equal to zero. In general, for projectiles with axial symmetry the moment is zero at $\psi = 0^\circ$, so that for equilibrium the projectile is oriented with its axis parallel to the direction of motion. If the projectile is rotated from the equilibrium position so as to give it a positive yaw angle, it is necessary that it have a negative moment coefficient, according to the sign convention adopted, in order that it be statically stable. Thus, a negative slope of the curve, C_M, vs. ψ corresponds to static stability, and a positive slope corresponds to instability. The degree of stability or instability is indicated by the magnitude of the slope. The same conclusions are obtained by interpreting the center-of-pressure curves. For symmetrical projectiles, if the center of pressure falls behind the center of gravity, a restoring moment exists and the projectile is statically stable. If the CP lies ahead of the CG, the moment is non-restoring and the projectile is statically unstable. The degree of stability or instability is indicated by the distance between the center of gravity and center of pressure.

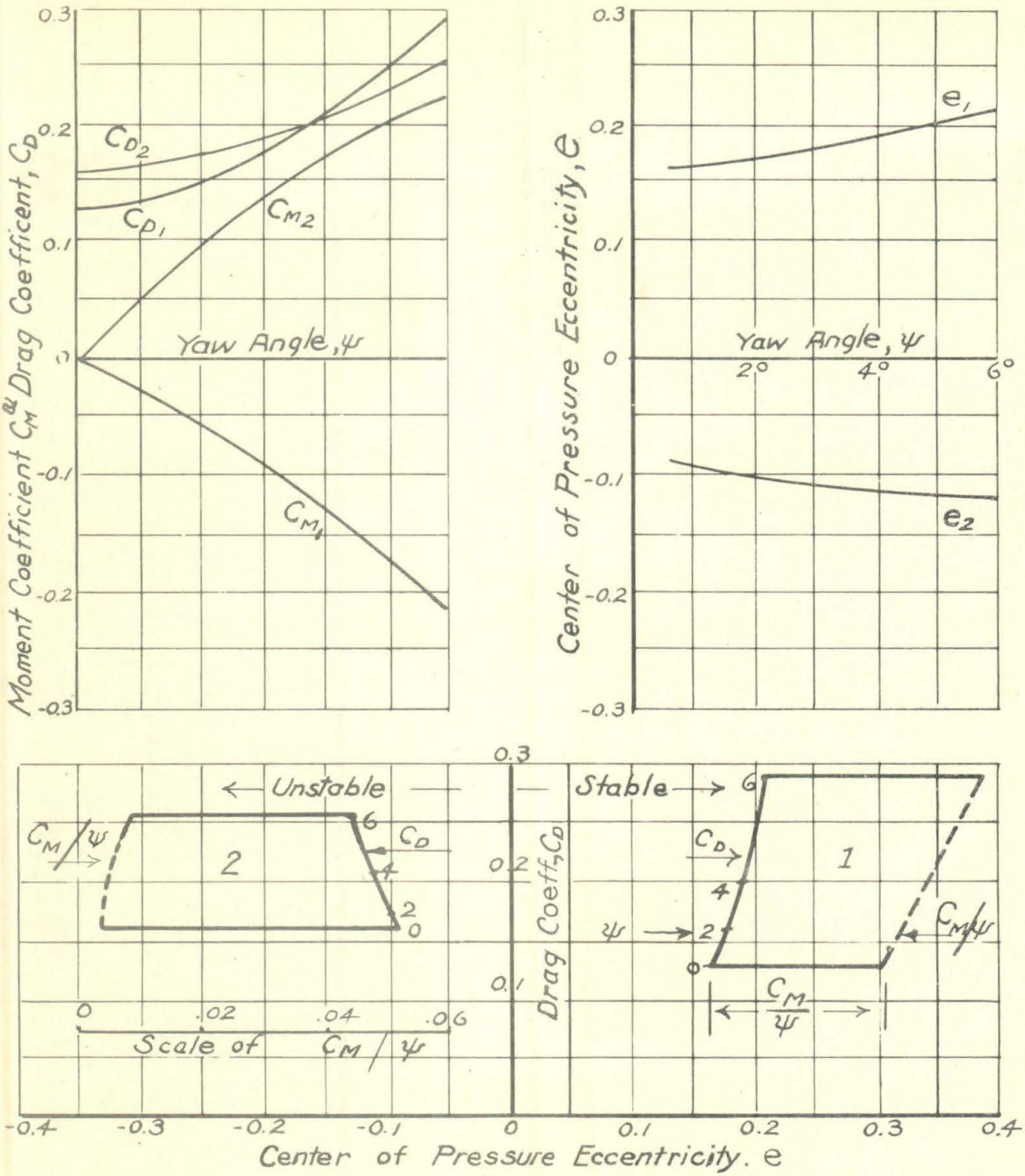

TYPICAL CHARACTERISTIC CHART

The California Institute of Technology---High Speed Water Tunnel.

ORG-M024-1671-L

THE HIGH SPEED WATER TUNNEL
AT THE
CALIFORNIA INSTITUTE OF TECHNOLOGY

APPENDIX B

DESCRIPTION OF CHARACTERISTIC CHART

The attached curve sheet shows typical curves for drag and moment coefficients and, also, center-of-pressure eccentricity, all varying with the yaw angle. Two cases have been assumed, indicated by the subscripts (1) and (2). These curves are selected merely to illustrate method of plotting the chart and do not represent data on the projectile discussed in this report.

In order to obtain a better visualization of the performance indicated by the curves mentioned above, the "Characteristic Chart", shown at the bottom of the sheet, has been devised. In this chart the drag coefficient, C_D, is first plotted against the CP eccentricity, e. On this C_D curve are points opposite which are figures indicating the yaw angle, ψ. This C_D curve shows the variation in drag and CP eccentricity with yaw angle. Also, the position of the curve at the right or left of the vertical axis (+ e or − e) indicates whether or not the projectile is stable or unstable, in other words, whether the CP lies aft or forward of the center of gravity.

On this same chart is plotted the quantity C_M/ψ which gives an indication of the change in the moment coefficient, C_M, with varying yaw angle. This is done by dividing the C_M by the yaw in degrees and plotting these values, C_M/ψ, to a suitable scale, horizontally from the points representing the yaw angle. (For each yaw angle the zero for the C_M/ψ scale is at the C_D curve).

The "Characteristic Chart" is useful as it gives a fairly complete picture of the variation of three important characteristics of the projectile with changes in yaw angle. It is seen that Case 1 has much less increase in drag than Case 2. Also, that the CP eccentricity in Case 1 increases with the yaw and is positive, and therefore, tends to increase stability. In addition to this, the C_M is increasing at an *increasing* rate, indicating a proportional increase in restoring moment with increasing yaw angles. This is an additional stabilizing factor.

In Case 2 the opposite characteristics of Case 1 are indicated. Here, there is a greater increase in drag with increase in yaw; also, the CP eccentricity, which is negative, increases with the yaw, thus tending to decrease stability. The change in moment coefficient occurs at a *decreasing* rate, indicating a proportional decrease in restoring moment with increasing yaw. This is a destabilizing factor.